Title	SMES control for power grid integrating renewable generation and electric vehicles
Author(s)	Gao, S; Chau, KT; Liu, C; Wu, D; Li, J
Citation	IEEE Transactions on Applied Superconductivity, 2012, v. 22 n. 3, p. 5701804:1-4
Issued Date	2012
URL	http://hdl.handle.net/10722/164050
Rights	Creative Commons: Attribution 3.0 Hong Kong License

SMES Control for Power Grid Integrating Renewable Generation and Electric Vehicles

Shuang Gao, K. T. Chau, Chunhua Liu, Diyun Wu, and Jiangui Li

Abstract—This paper presents a superconducting magnetic energy storage (SMES) control system for the power distribution grid which integrates renewable generation and electric vehicles (EVs) together. Based on a 33-bus 4-lateral radial distribution system, coordinated control is developed. With the use of SMES, any transient unbalance caused by wind power variation can be recovered so that the system frequency can be stabilized. Also, with the use of EVs, the steady-state load demand can be redistributed to facilitate the adoption of wind power generation. Finally, simulation results verify that the use of both SMES and EVs can effectively perform power balancing under both the transient and steady states.

Index Terms—Electric vehicles, frequency regulation, load regulation, power grid, renewable generation, superconducting magnetic energy storage (SMES).

I. INTRODUCTION

T O COPE with global energy crisis and environmental pollution, renewable generation especially wind power [1] is becoming desirable to integrate into the existing power grid [2], while electric vehicles (EVs) especially the plug-in hybrid EVs (PHEVs) are becoming attractive for green transportation [3]. Because of the intermittent nature of wind power, it is a challenge to maintain both transient and steady-state balances of the power grid. Recently, the superconducting magnetic energy storage (SMES) has been introduced to alleviate the problem of power imbalance [4].

With ever increasing popularity of PHEVs, the vehicle-to-grid (V2G) operation provides an opportunity to utilize the energy stored in vehicle batteries as distributed power plants. Namely, the PHEVs not only draw power from the grid to charge batteries, but can also feed power back to the grid when necessary.

In this paper, the SMES is incorporated into the power system having wind power units and PHEVs. Then, a coordinated control algorithm is proposed to perform both load and frequency regulations. Simulation results will be given to verify the validity of the proposed system and algorithm.

II. SYSTEM MODELING

Fig. 1 shows a 33-bus 4-lateral radial distribution system which includes 2 SMES units, 2 wind power units and 6
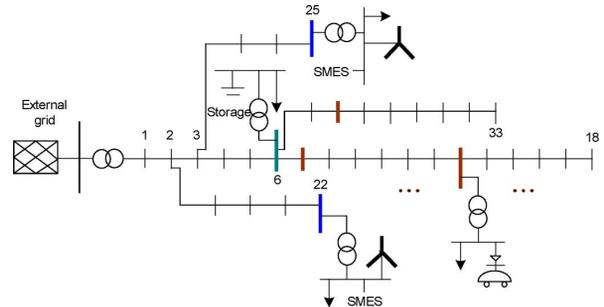
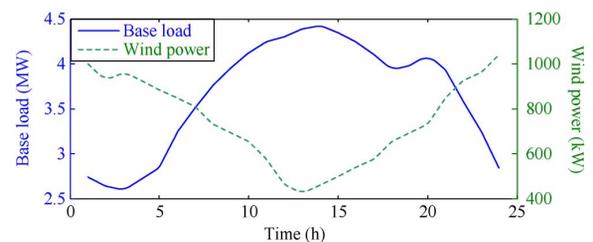Fig. 1. Proposed distribution system.

Fig. 2. Profiles of base load and wind power.

PHEV units. Initially, the capacity of wind power generation is selected as 20% of the total generation capacity installed [5] while the capacity of PHEVs is set to 10% of the total load demand [6], which are the near-term targets for modern cities. The daily profiles of base load and wind power are depicted in Fig. 2. It can be observed that the wind power cannot directly relieve the base load without energy storage, since the crest of base load generally coincides with the trough of wind power.

The wind power units are modeled as fixed-speed wind turbines [7]. They include two types of power converters, namely the AC-DC and DC-AC, for the desired voltage conversion. The PHEV units comprise of PHEVs and bidirectional DC-AC converters. Since each PHEV may not offer sufficient energy storage for V2G operation, an aggregator is used to represent a group of PHEVs. And the storage capacity of the PHEV aggregation can be determined based on the capacity of their on-board battery packs.

The control strategy for the SMES units has three main functions: namely, the frequency compensation control which detects the frequency fluctuation of the load and generates the reference value for the converter; the converter system control which regulates the power output of SMES; and the DC-DC chopper control which coordinates the power transfer according to the reference power output.

III. COORDINATED CONTROL

In the proposed distribution system, the energy from all sources and loads are coordinated to perform power balancing and frequency control. This coordinated control comprises of

two parts: the hourly time scale and the secondly time scale. In the hourly time scale, the EV charging and discharging are controlled to reform the load profile. In the secondly time scale, the SMES system is used to compensate the transient fluctuation of wind power generation.

In order to devise the sizes of SMES and PHEVs with respect to the level of wind power generation, the average wind power generation P_{WT}, the average PHEV charging power P_{EV} and the SMES power capacity P_{SM} are governed by:

$$P_{WT} = k_{WT} P_{BL} \tag{1}$$
$$P_{EV} = k_V P_{WT} = k_V k_{WT} P_{BL} \tag{2}$$
$$P_{SM} = k_{\mathrm{M}} P_{WT} = k_M k_{WT} P_{BL} \tag{3}$$

where P_{BL} is the average power demand of the daily load profile, k_{WT} is the proportional constant of the wind power to the load demand, k_V is the proportional constant of PHEV charging power to the wind power, and k_M is the proportional constant of SMES power capacity to the wind power. Since the PHEV serves for the steady-state power balancing while the SMES for the transient power balancing, their energy storage capacities should satisfy the wind energy fluctuation as governed by:

$$P_{EV} T + \int p_{SM} dt > a_p \int p_{WT} dt \tag{4}$$

where T is the charging period of PHEVs, p_{SM} is the instantaneous SMES power output, p_{WT} is the instantaneous wind power generation, and a_p is the coefficient of the available energy constraint provided by PHEVs and SMES. It actually shows the minimum PHEV and SMES storage capacities that can mitigate the fluctuation effect of wind power generation.

Since the SMES is designed to perform transient stabilization of the power grid, the corresponding energy capacity E_{SM} and power capacity P_{SM} need to satisfy the following criteria:

$$E_{SM} > a_f (\max(p_{WT}(t) - p_{WT}(t - \Delta T)) \Delta T \tag{5}$$
$$P_{SM} > b_f (P_{WT,\max} - P_{WT,\min}) \tag{6}$$
$$\Delta p_{SM} / \Delta t > c_f [\max(p_{WT}(t) - p_{WT}(t - \Delta t) / \Delta t)] \tag{7}$$

where p_{WT} is the wind generator power output at time t, ΔT is the time interval of wind power fluctuation, a_f is the coefficient of the SMES energy capacity constraint, $P_{WT,max}$ and $P_{WT,min}$ are respectively the maximum and minimum values of wind power fluctuation, b_f is the coefficient of the SMES power capacity constraint, Δp_{SM} is the change of SMES power, Δt is the time interval to assess the rate of change of SMES power, and c_f is the coefficient of the SMES power adjustment rate constraint.

The boundary conditions for the PHEVs to perform load regulation of the power grid are given by:

$$\int p_{EVi}(t) dt = E_{EVi,\max} - E_{EVi,\text{int}} \tag{8}$$
$$E_{V2G} / E_{EV} \leq r_{V2G} \tag{9}$$

where $p_{EVi}(t)$ is the charging or discharging rate of the PHEV aggregation i, $E_{EVi,max}$ and $E_{EVi,int}$ are respectively the maximum and initial energy storages of the PHEV aggregation i at the end and beginning of the charging period, E_{V2G} is the energy that is discharged from PHEV batteries back to the power grid, E_{EV} is the energy required to fully charge PHEVs, and r_{V2G} is the V2G ratio which is defined as the ratio of the energy fed back to the power grid by discharging the PHEVs to the energy drawn from the power grid for charging the PHEVs.

The boundary conditions for the SMES to perform frequency regulation of the power grid are given by:

$$P_{SM,\min} \leq p_{SM}(t) \leq P_{SM,\max} \tag{10}$$
$$0 \leq E_{SM,\text{int}} + \int p_{SM}(t) dt \leq E_{SM} \tag{11}$$

where $P_{SM,min}$ and $P_{SM,max}$ are respectively the lower and upper bounds of SMES power output, and $E_{SM,int}$ is the initial energy storage of the SMES. The operational power $p_{SM}(t)$ can be produced only within the energy limit of E_{SM}.

The coordinated control method [8] is attractive for V2G operation which can optimize the load regulation of the power grid [9]. In this paper, this method is extended to minimize the total power losses under the hourly time scale and to minimize the grid frequency fluctuation under the secondly time scale. The overall objective function F_o is defined as:

$$F_o(p_{EV}(t_H), p_{SM}(t_S), p_{WT}(t)) = \min(w_l F_l + w_f F_f) \tag{12}$$

where t_H is the time under hourly time scale, t_S is the time under secondly time scale, w_l is the weight for load regulation, w_f is the weight for frequency regulation, F_l is the function for load regulation and F_f is the function for frequency regulation. The corresponding weights are expressed as:

$$\begin{cases} w_l = (\Delta t - \Delta t_f) / \Delta t \\ w_f = \Delta t_f / \Delta t \end{cases} \tag{13}$$

where Δt is the time interval for simulation, and t_f is the reference value of time interval for simulation. The values of w_l and w_f are restricted to the interval between 0 and 1. Meanwhile, the corresponding functions are expressed as:

$$F_l = \sum_{k=1}^{T_H} \sum_{j=1}^{L} I_j^2 (p_{EV}(t_{Hk}), p_{SM}(t_{Sk}), p_{WT}(t_k)) l_j \Delta t_H \tag{14}$$
$$F_f = \sum_{i=1}^{n_{WT}} \sum_{k=1}^{T_S} \Delta f_i (p_{EV}(t_{Hk}), p_{SM}(t_{Sk}), p_{WT}(t_k)) \tag{15}$$

where I_j and l_j are respectively the current and resistance of the transmission line j during the time interval Δt_H of load regulation, L is the number of transmission lines, T_H is the whole V2G operation period under the hourly time scale, Δf_i is the grid frequency variation at the wind generator i, T_S is the operation period for frequency regulation under the secondly time scale, and n_{WT} is the number of wind generators in the grid.

Due to the nature of short-term energy storage of the SMES, $p_{SM}(t_{Sk})$ in (14) during the large time interval Δt_H is ignorable. Meanwhile, since repetitive PHEV charging is not possible within a short time period, $p_{EV}(t_{Hk})$ in (15) can also be omitted. Hence, the objective function given by (12)–(15) can be further simplified.

Consequently, the proposed power distribution grid incorporating wind power generation, PHEVs and SMES as well as the proposed coordinated control algorithm are analysed using MATLAB simulation. The key simulation parameters,

TABLE I
SIMULATION PARAMETERS

Grid parameters		System parameters	
$P_{i,max}$	420 kW	k_{WT}	0.2
$P_{i,min}$	60 kW	k_V	0.5
$Q_{i,max}$	600 kVar	k_M	0.2
$Q_{i,min}$	20 kVar	a_p	0.2
$R_{l,max}$	1.068 p.u.	a_f	0.5
$R_{l,min}$	0.0575 p.u.	b_f	0.5
$X_{l,max}$	0.8457 p.u.	c_f	1
$X_{l,min}$	0.0393 p.u.	Δt_f	1 s
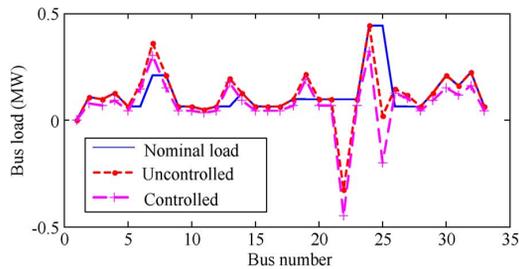
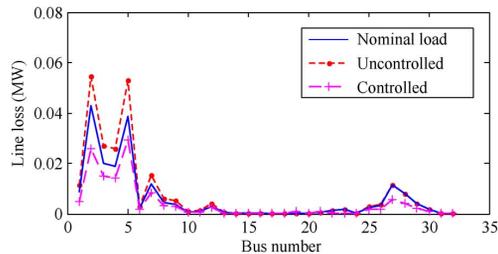Fig. 3. Bus load distributions with and without coordinated control.

Fig. 4. Line losses at various buses with and without coordinated control.

including the standard 33-bus distribution grid parameters and the system parameters, are listed in Table I.

IV. SIMULATION RESULTS

A. Steady-State Regulation

Fig. 3 shows the distribution of nominal load, namely the base load plus wind power generation, as well as the distributions of nominal load plus PHEV load under uncontrolled and controlled operations. The uncontrolled operation refers to the standard charging of PHEVs, whereas the controlled operation refers to the PHEV load under the proposed coordinated control. It can be seen that the use of coordinated control can effectively reduce the peaky bus load at the 6 buses with PHEVs connected. Also, the use of coordinated control can significantly reduced the power losses on the transmission lines as shown in Fig. 4. Line loading rate is an important limiting factor for accommodating higher load demand. The maximum line loading can be reduced by a third so that a higher level of PHEV penetration is allowed.

Since all the PHEVs should be charged up before each daily usage, the charging period is set from evening 6 pm to next
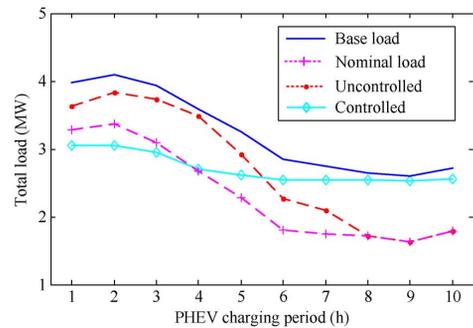

Fig. 5. Load profiles with and without coordinated control.
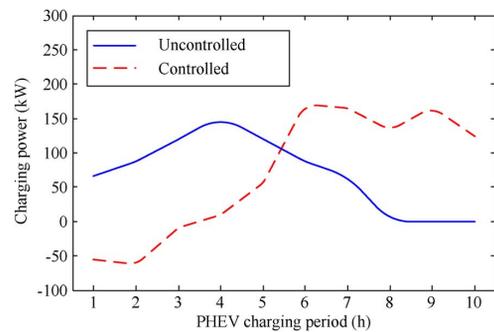

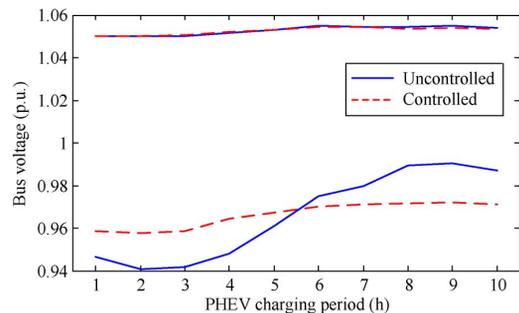Fig. 6. PHEV charging power profiles with and without coordinated control.

Fig. 7. Bus voltage range profiles with and without coordinated control.

morning 5 am (totally 10 h). The nominal load as well as the nominal load plus uncontrolled PHEV load are plotted in Fig. 5 which indicates that heavy load occurs at first few hours whereas light load occurs at last few hours. Notice that the load fluctuation of the nominal load is larger than that of the base load, which agrees with the realistic profiles shown in Fig. 2 that the wind power is almost anti-phase with the base load. In the presence of coordinated control, the load profile can be effectively leveled. The charging and discharging rate of each PHEV aggregation is varied according to the solutions of optimal control algorithm. At a particular bus, both the uncontrolled and controlled PHEV charging loads are plotted together in Fig. 6. It can be observed that the controlled PHEVs feed power back to the grid in first few hours, thus confirming the use of V2G operation under coordinated control. Moreover, the maximum and minimum bus voltages with and without using coordinated control are plotted together in Fig. 7. It confirms that the use of coordinated control can curtail the bus voltage drop to less than 5% of the nominal value.
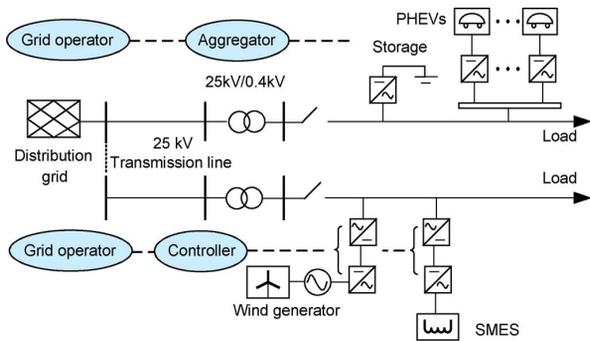
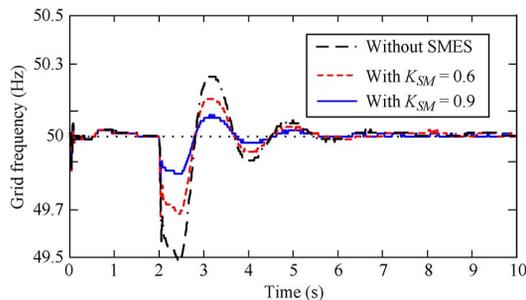Fig. 8. Micro-grid architecture involving wind generator, SMES and PHEVs.

Fig. 9. Frequency profile with and without the SMES system.

Fig. 10. Response of the SMES to the sudden change in the wind power.

B. Transient Regulation

Due to low storage capacity, the SMES unit cannot perform as a power source or load to level the hourly load profiles. Nevertheless, it can be used to effectively stabilize the grid frequency in the transient state. As shown in Fig. 8, the SMES unit is connected to the bus of the wind generator so as to directly compensate the power discrepancy due to the wind speed variation.

As aforementioned, the energy and power capacities of SMES are sized by using (5)–(7). Particularly, the parameter a_f indicates the minimum amount of SMES energy capacity for the system. In order to assess the most appropriate amount of SMES energy capacity for satisfying the constraint of grid frequency variation, a SMES index K_{SM} is defined as:

$$K_{SM} = \frac{E_{SM}}{\left(\max\left(p_{WT}(t) - p_{WT}(t - \Delta T)\right)\Delta T\right)} > a_f \quad (16)$$

where ΔT is the time interval that the SMES unit is activated to compensate the maximum power fluctuation of the wind generator.

Under the same condition of wind power fluctuation, the grid frequency profiles with and without using the SMES unit are shown in Fig. 9. It can be found that the grid frequency swings below 49.5 Hz in the absence of SMES, which is not acceptable for normal power distribution grid. On the contrary, when adopting the SMES system with $K_{SM} = 0.6$ or $K_{SM} = 0.9$, the frequency variation can be significantly suppressed. Fig. 10 depicts the corresponding SMES power under $K_{SM} = 0.6$, confirming that the SMES unit can instantaneously release and absorb power to stabilize the transient fluctuation. Moreover, it can be found that the SMES unit with $K_{SM} = 0.6$ is sufficient
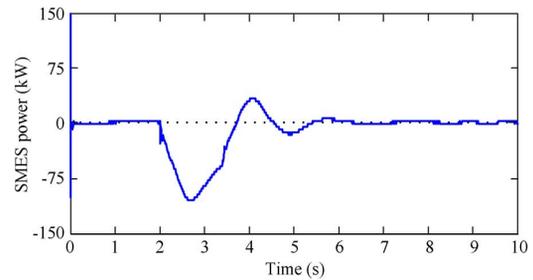
to suppress the frequency fluctuation less than 0.5 Hz. From this aspect, the SMES system with $K_{SM} = 0.9$ is overdesigned and its energy capacity is superfluous.

V. CONCLUSION

In this paper, a modern power distribution grid incorporating wind power generation, PHEVs and SMES has been presented. A coordinated control method of SMES and V2G operation has been proposed to perform power balancing of the grid under both steady and transient states. Namely, with the use of PHEV aggregation to perform V2G operation, the steady-state load demand can be redistributed to compensate the variation of wind power generation. Meanwhile, with the use of SMES to supply and absorb transient power, the transient frequency fluctuation can be effectively stabilized. The simulation results verify that the proposed power distribution grid and the proposed coordinated control can provide effective load regulation and frequency stabilization in the presence of intermittent wind power generation.

REFERENCES

[1] C. Liu, K. T. Chau, and J. Z. Jiang, "Design of a new outer-rotor permanent-magnet hybrid machine for wind power generation," *IEEE Trans. Magn.*, vol. 44, no. 6, pp. 1494–1497, 2008.

[2] C. Liu, K. T. Chau, and X. Zhang, "An efficient wind-photovoltaic hybrid generation system using doubly-excited permanent-magnet brushless machine," *IEEE Trans. Ind. Electron.*, vol. 57, no. 3, pp. 831–839, 2010.

[3] K. T. Chau and C. C. Chan, "Emerging energy-efficient technologies for hybrid electric vehicles," *Proceedings of IEEE*, vol. 95, no. 4, pp. 821–835, 2007.

[4] A. R. Kim, H. Seo, G. Kim, M. Park, I. Yu, Y. Otsuki, J. Tamura, S. Kim, K. Sim, and K. Seong, "Operating characteristic analysis of HTS SMES for frequency stabilization of dispersed power generation system," *IEEE Trans. Applied Supercond.*, vol. 20, no. 3, pp. 1334–1336, 2010.

[5] Database of State Incentives for Renewables and Efficiency [Online]. Available: http://www.dsireusa.org/incentives/index.cfm

[6] C. D. White and K. M. Zhang, "Using vehicle-to-grid technology for frequency regulation and peak-load reduction," *J. Power Sources*, vol. 196, no. 8, pp. 3972–3980, 2011.

[7] P. S. Moura and A. T. Almeida, "The role of demand-side management in the grid integration of wind power," *Applied Energy*, vol. 87, no. 8, pp. 2581–2588, 2010.

[8] S. Gao, K. T. Chau, C. C. Chan, C. Liu, and D. Wu, "Optimal control framework and scheme for integrating plug-in hybrid electric vehicles into grid," *J. Asian Electric Vehicles*, vol. 9, no. 1, pp. 1473–1481, 2011.

[9] S. Gao, K. T. Chau, C. C. Chan, and D. Wu, "Loss analysis of vehicle-to-grid operation," in *IEEE Vehicle Power and Propulsion Conference*, Lille, 2010, pp. 1–6.